



Discriminative MRI Findings of Pituitary Adenomas from Craniopharyngiomas

Hipofiz Adenomlarının Kraniyofarinjiomlardan Ayırıcı MRG Bulguları

Elmire Dervişoğlu¹*, Ceylan Altıntaş¹*, İsa Çam¹*, Burak Çabuk²*, İhsan Anık²*,
Savaş Ceylan²*, Yonca Anık¹*

¹Kocaeli University, Faculty of Medicine, Department of Radiology, Kocaeli, Turkey.

²Kocaeli University, Faculty of Medicine, Department of Neurosurgery, Kocaeli, Turkey.

Atf/Cite as: Dervişoğlu E, Altıntaş C, Çam İ, et al. Discriminative MRI Findings of Pituitary Adenomas From Craniopharyngiomas. J Nervous Sys Surgery 2022;8(3):94-103.

Geliş tarihi/Received: 07.11.2022 **Kabul tarihi/Accepted:** 24.11.2022 **Yayın tarihi/Publication date:** 21.12.2022

ABSTRACT

Purpose: The aim of this study is to determine and define differential magnetic resonance imaging (MRI) findings of pituitary adenomas and craniopharyngiomas.

Materials and methods: This retrospective analysis was performed on MR imaging findings of 45 pituitary adenomas and 41 craniopharyngiomas with solid and cystic mixed appearance. MRI findings including shape ovoid, snowman, lobulation, chiasma compression, cavernous sinus invasion, 3rd ventricle compression, calcification, predominant type – cystic vs solid, contrast enhancement patterns – homogenous, reticular and extension were assessed.

Results: Among MRI findings superiorly lobulated shape, third ventricle compression and reticular enhancement of solid parts were common in craniopharyngiomas while snowman shape, predominantly solid content, homogenous enhancement of solid parts were compatible with adenomas significantly at $p < 0.05$ for all.

Conclusion: Tumor shape and contrast enhancement patterns of solid parts seem discriminative MRI features for pituitary adenoma and craniopharyngiomas.

Keywords: Pituitary adenoma, craniopharyngioma, magnetic resonance imaging

ÖZ

Amaç: Bu çalışmanın amacı hipofiz adenomları ve kraniyofarenjiyomların ayırıcı manyetik rezonans görüntüleme (MRG) bulgularını belirlemek ve tanımlamaktır.

Gereç ve yöntem: Bu retrospektif analiz, solid ve kistik mikst görünümde 45 hipofiz adenomu ve 41 kraniyofarenjiyomun MR görüntüleme bulguları üzerinde yapıldı. Ovoid şekil, kardan adam şekli, lobülasyon,

Sorumlu yazar/Corresponding author: İhsan Anık, Kocaeli University, Faculty of Medicine, Department of Neurosurgery, Kocaeli, Turkey.

drianik@yahoo.com / 0000-0003-2567-7969

ORCID:

E. Dervişoğlu 0000-0002-2431-048X, **C. Altıntaş** 0000-0003-4459-4114, **İ. Çam** 0000-0001-9551-2364, **B. Çabuk** 0000-0003-1198-3869, **S. Ceylan** 0000-0002-2747-8907, **Y. Anık** 0000-0002-6768-2574

© Telif hakkı Sinir Sistemi Cerrahisi Dergisi.

Bu dergide yayınlanan bütün makaleler Creative Commons 4.0 Uluslararası Lisansı (CC-BY) ile lisanslanmıştır.

© Copyright Journal of Nervous System Surgery.

Licensed by Creative Commons Attribution 4.0 International (CC BY).

kiazma kompresyonu, kavernöz sinüs invazyonu, 3. ventrikül kompresyonu, kalsifikasyon, baskın tip – kistik vs katı, kontrast tutma paternleri – homojen, retiküler ve ekstansiyon gibi MRG bulguları değerlendirildi.

Bulgular: MRG bulguları arasında lobüle şekil, üçüncü ventrikül kompresyonu ve solid kısımların retiküler kontrastlanması kraniyofarenjiomlarda yaygın iken, kardan adam şekli, ağırlıklı olarak solid içerik, solid kısımların homojen kontrastlanması adenomlarda anlamlı bulgu olarak $p<0.05$ 'te uyumlu bulundu.

Sonuç: Tümör şekli ve solid kısımların kontrastlanma paternleri, hipofiz adenomu ve kraniyofarenjiomlar için anlamlı ayırt edici MRG özellikleri olarak görülmüştür.

Anahtar Kelimeler: Hipofiz adenomu, kraniyofarenjiyom, manyetik rezonans görüntüleme

INTRODUCTION

Pituitary adenomas are benign epithelial lesions and account for about 10–15% of all intracranial tumors representing the most common intrasellar pathology and the most common lesions involving both intrasellar and suprasellar regions⁽¹⁾. An uncomplicated pituitary adenoma is isointense to grey matter on T1 and T2 weighted magnetic resonance imaging (MRI), and shows homogeneous enhancement pattern after contrast administration⁽²⁻⁴⁾. When a pituitary adenoma is complicated with necrosis, hemorrhage and cystic degeneration, it shows various signal intensity and enhancement pattern that can be similar with craniopharyngioma⁽²⁻⁴⁾.

Craniopharyngiomas are neoplasms arising from squamous epithelial cell rests of Rathke's pouch. Typical appearance of a craniopharyngioma is a mixed cystic and solid mass in suprasellar region. Cystic component usually shows high signal intensity on T1-weighted images. Intrasellar involvement by a large craniopharyngioma is found in about 20-25%⁽⁵⁾.

When a lesion involves both intrasellar and suprasellar regions, the differential diagnosis is important because surgical planning depends on it. While pituitary adenomas are usually approached by the transsphenoidal route, craniopharyngiomas require craniotomy and radical surgery⁽⁶⁻⁸⁾.

In this study, we aimed to investigate the differential MRI findings of mixed cystic-solid pituitary adenomas and craniopharyngiomas involving both intrasellar and suprasellar regions.

METHODS

Study population

This retrospective study was approved by Kocaeli University institutional review board. We retrospectively reviewed pituitary MR imaging and electronic medical records in our center between 2010 and 2018.

The inclusion criteria were as follows: (a) both sellar and suprasellar involvement, (b) mixed cystic-solid character, (c) histopathologically proven adenoma or craniopharyngioma and the exclusion criteria were: (a) the mass involved only sellar or suprasellar region, (b) pure solid or pure cystic character, (c) any mass except from adenoma or craniopharyngioma.

86 patients with pituitary adenoma (n=45) and craniopharyngioma (n=41) were included in the study. Patients' ages ranged between 28 and 66 years (mean 44 years) for adenomas, and between 2 and 63 years (mean 30 years) for craniopharyngiomas. Forty-seven patients were men (22 adenoma, 25 craniopharyngioma) and 39 patients were women (23 adenoma, 16 craniopharyngioma). Demographic data of patients are shown in Table 1.

Table 1. Demographic data of patients.

		Pituitary adenoma (n=45)	Craniopharyngioma (n=41)	p value
Sex	Female	23	16	0.616
	Male	22	25	0.616
Age	Mean (SD)	44 (9.7)	30(21)	0.001

MRI protocols

MR images were obtained using 1.5 Tesla MRI (Gyrosan Intera, Philips Medical Systems, Eindhoven, The Netherlands) and 3 Tesla MRI (Achieva Interna: Philips Medical Systems, Eindhoven, The Netherlands) scanners in our center, using a 16-channel head coil.

Sagittal fat-saturated precontrast T1W images were acquired on both MRIs with TE 15 ms, TR 570 ms; coronal T2W images were acquired with TE 120 ms, TR 3000 ms; precontrast coronal and sagittal T1W images were acquired with TE 10 ms, TR 500 ms. All sequences were performed with a slice thickness of 3 mm, a gap of 0.3 mm, and a FOV of 120 mm. Dynamic coronal T1W images were obtained on both MRIs with TE 10 ms, TR 500 ms with a slice thickness of 2 mm, a gap of 0.2 mm, and a FOV of 120 mm three minutes following the injection of contrast agent.

MRI assesment

All MRI images were reviewed on a picture archiving and communication system (PACS) workstation. Two radiologists evaluated MRI findings by consensus.

Tumour shapes were classified as ovoid, snowmanlike, or superiorly lobulated. A snowman shape was defined as a figure of eight-like shape, and superiorly lobulated shape as having two or more lobes in the suprasellar compartment.

Superior extensions were graded as below the optic chiasm, compressing the optic chiasm, and compressing the third ventricle. Compression of the third ventricle was considered to occur if the

third ventricle floor was indented. A lateral extent was classified as one within or beyond the lateral margin of the cavernous intracranial carotid artery (ICA).

Tumour characteristics were classified as predominantly solid or predominantly cystic. Signal intensities of the solid portion of tumours on T2-weighted MRI images were classified as hyperintense (higher than the signal intensity of grey matter) or not. Signal intensities of the cystic portion of tumours on T1-weighted MRI images were also classified as hyperintense (higher than the signal intensity of whiter matter), or not. Enhancement patterns of solid portions were classified as homogeneous or reticular (mesh-like enhancements with intervening non-enhancing tiny defects).

Statistical analysis

All statistical analyses were performed using the IBM SPSS 20.0 (SPSS Inc., Chicago, IL, USA). Numerical variables were expressed as mean +/- standard deviation and categorical variables were expressed as frequency (percentage). The normality of the data distribution was evaluated by the KolmogorovSmirnov test. Numerical variables were evaluated using Student's t tests since the normal distribution was achieved. The relationship between categorical variables was evaluated by χ^2 -test. $p < 0.05$ was considered statistically significant.

RESULTS

The MRI features of pituitary adenoma, and craniopharyngioma are summarized in the Table 2. The most common shape of pituitary adenomas was snowman (Fig. 1 and 2) appearance (55.6%, 25 of 45 patients), while the most common shape of craniopharyngiomas was superior lobulation (Fig. 3 and 4) (78%, 32 of 41 patients). There was statistically significant difference between groups ($p < 0.001$).

Table 2. The MRI features of pituitary adenoma, and craniopharyngioma are summarized.

	MRI features	Pituitary adenoma (n=45)	Craniopharyngioma (n=41)	p value
Shape	Ovoid	11 (24.4%)	5 (12.2%)	0.337
	Snowman-like shape	25 (55.6%)	4 (9.8%)	<0.001
	Superior lobulation	9 (20%)	32 (78%)	<0.001
Component characteristics	Predominantly solid	18 (40%)	11 (26.8%)	0.024
	Predominantly cystic	27 (60%)	30 (73.2%)	0.287
Signal intensity	T2 hyperintense solid component	9 (20%)	9 (22%)	0.949
	T1 hyperintense cystic portion	17 (38%)	25 (61%)	0.102
Extension	Compressing optic chiasm	36 (80%)	34 (82.9%)	1.000
	Compressing third ventricle	14 (31.1%)	29 (70.7%)	0,003
	Cavernous sinus invasion	10 (22.2%)	1 (2.4%)	0,011
Enhancement pattern of solid portion	Homogeneous	42 (93.3%)	5 (12.2%)	<0.001
	Reticular	3 (6.7%)	36 (87.8%)	<0.001

There was no statistically significant difference in the signal intensity of the solid portion on T2 weighted images between pituitary adenoma and craniopharyngioma ($p=0.949$). Also, in terms of the signal intensity of the cystic portion on T1-weighted images, although the high

signal intensity of the cystic portion was more frequently observed in craniopharyngioma (Fig. 4 and 6) (61%, 25 of 41 patients) than in pituitary adenoma (Fig. 2 and 5), there was no statistically significant difference ($p=0.102$).

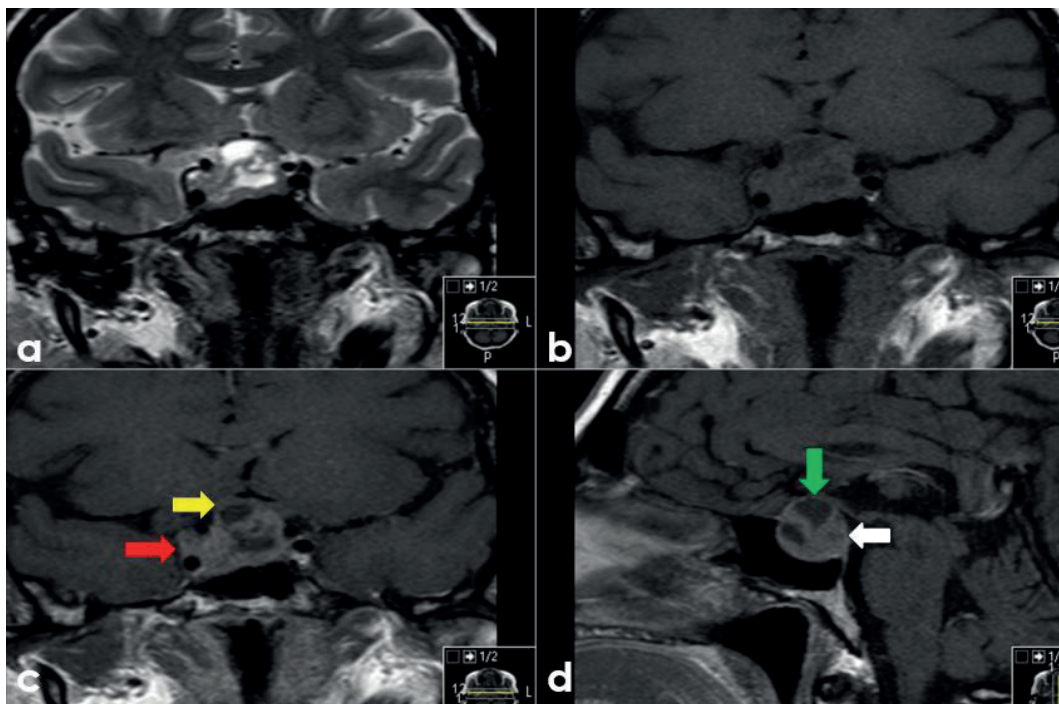


Figure 1. Pituitary adenoma in a 45-year-old woman with a snowman-like shape, homogeneously enhancing solid portion (white arrow in d) and T1 hypointense cystic portion (green arrow in d). The superior portion compresses the optic chiasm (yellow arrow in c). Also it invades the right cavernous sinus (red arrow in c).

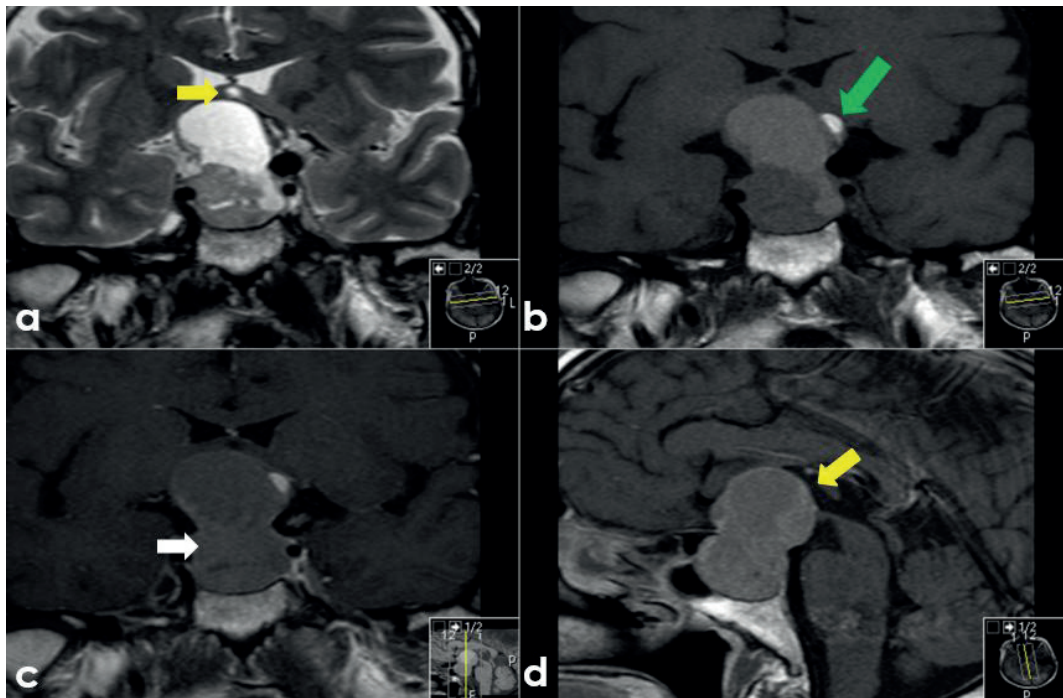


Figure 2. Pituitary adenoma in a 53-year-old male patient with a snowman-like shape, T1 hyperintense cystic portion (green arrow in b) and homogeneously enhancing solid portion (white arrow in c). The superior portion compresses the third ventricle floor (yellow arrows in a and d).

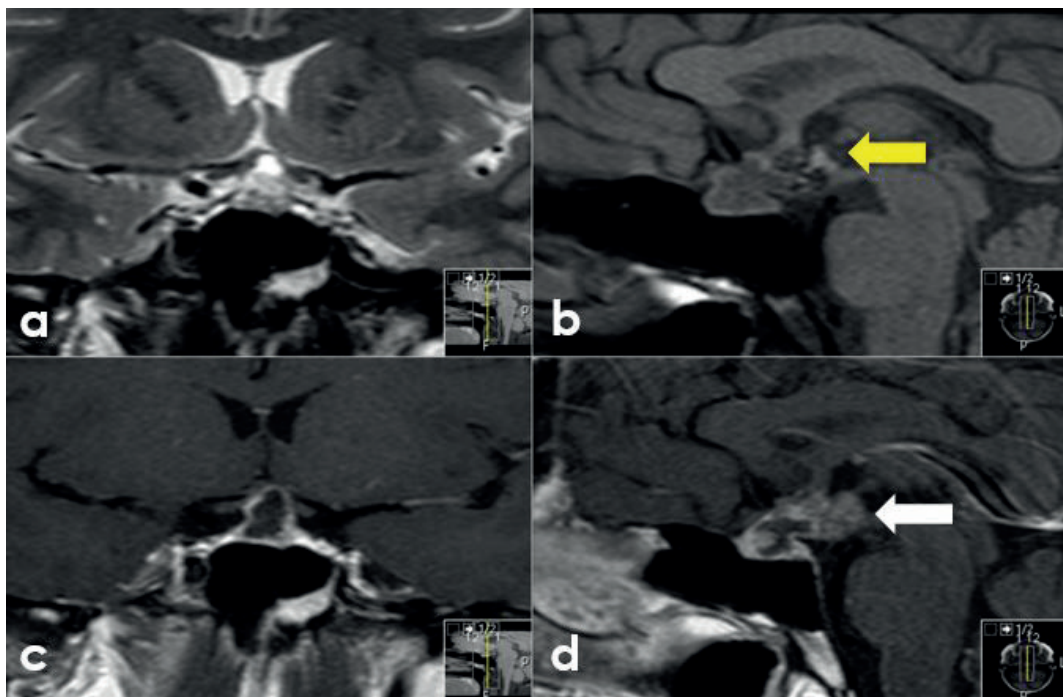


Figure 3. Craniopharyngioma in a 32-year-old male patient with a superior lobulated shape, and heterogeneously enhancing solid portion (white arrow in d). The superior portion compresses the third ventricle floor (yellow arrow in b).

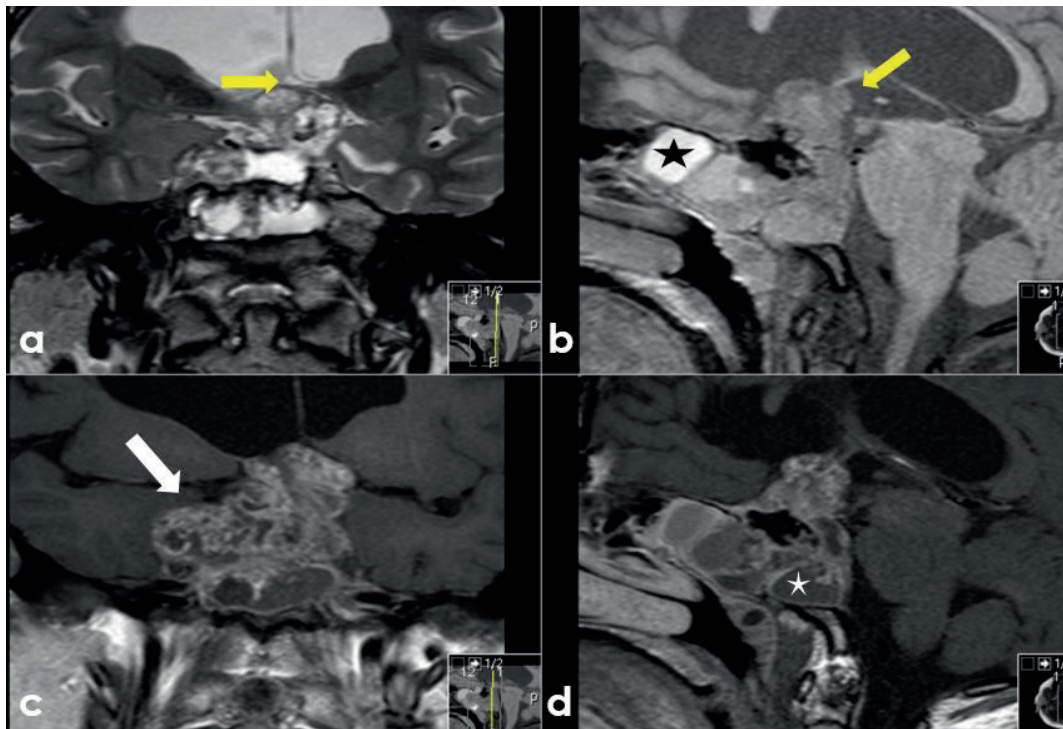


Figure 4. Craniopharyngioma in a 20-year-old male patient with a superior lobulated shape, T1 hyperintense (black star in b) and hypointense (white star in d) cystic portions and heterogeneously enhancing solid portion (white arrow in c). The superior portion compresses the third ventricle floor (yellow arrows in a and b).

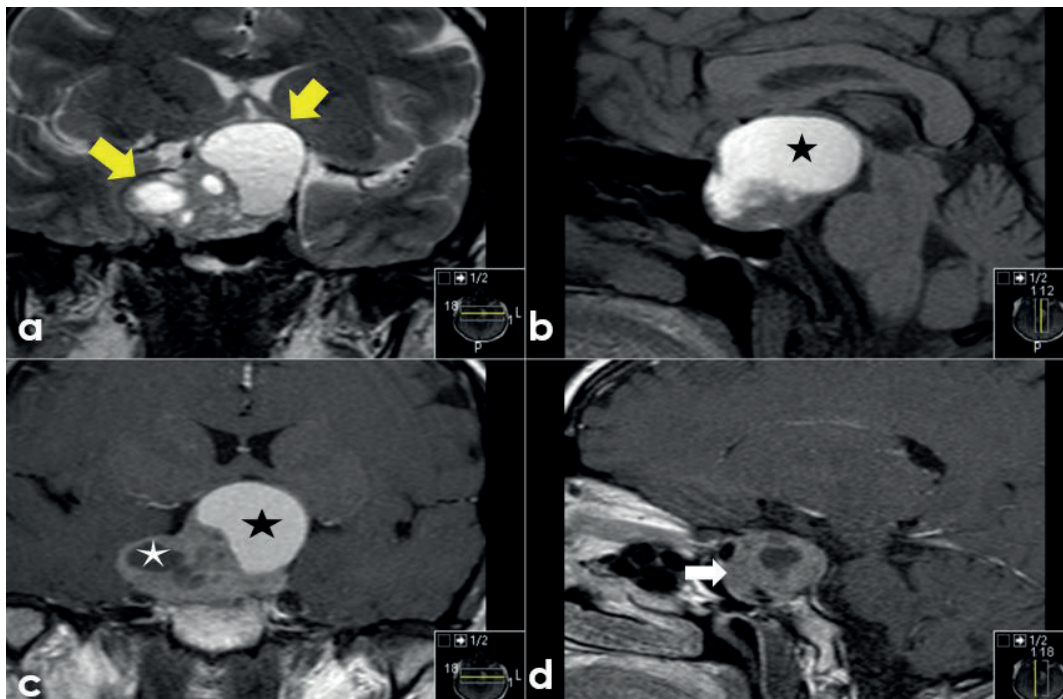


Figure 5. Pituitary adenoma in a 34-year-old female patient with a superior lobulated shape (yellow arrows in a), T1 hyperintense (black stars in b and c) and hypointense (white star in c) cystic portions and homogeneously enhancing solid portion (white arrow in d).

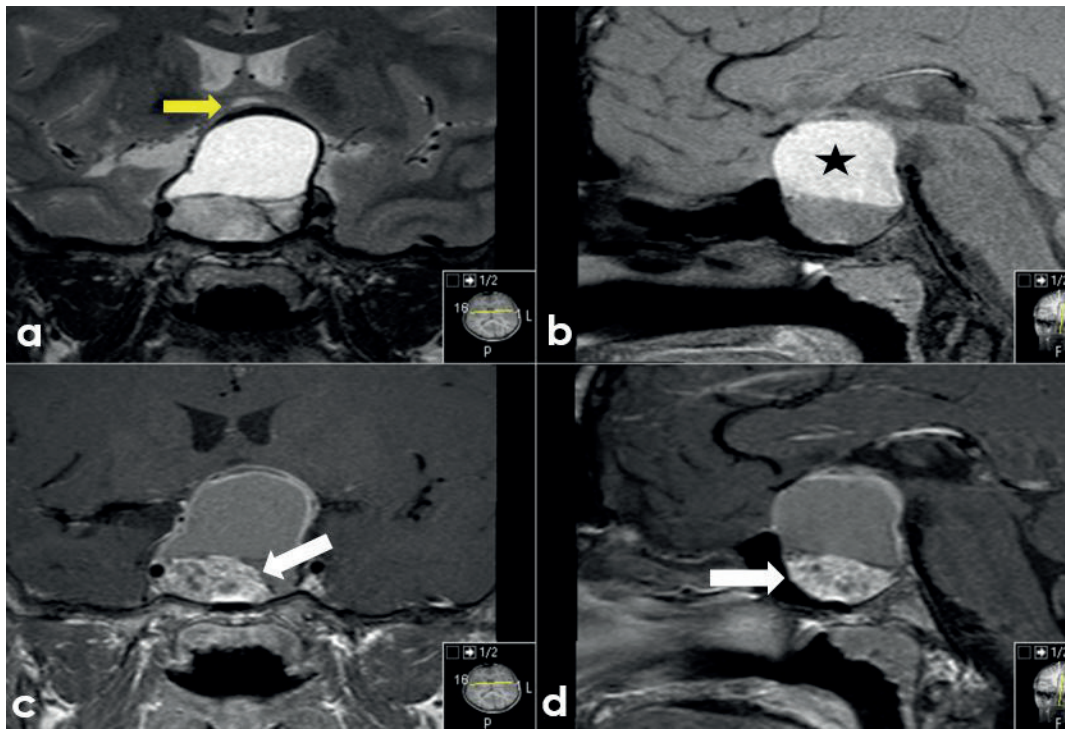


Figure 6. Craniopharyngioma in a 14-year-old female patient with a snowman-like shape, T1 hyperintense cystic portion (black star in b) and heterogeneously enhancing solid portion (white arrows in c and d). The superior portion compresses the third ventricle floor (yellow arrow in a).

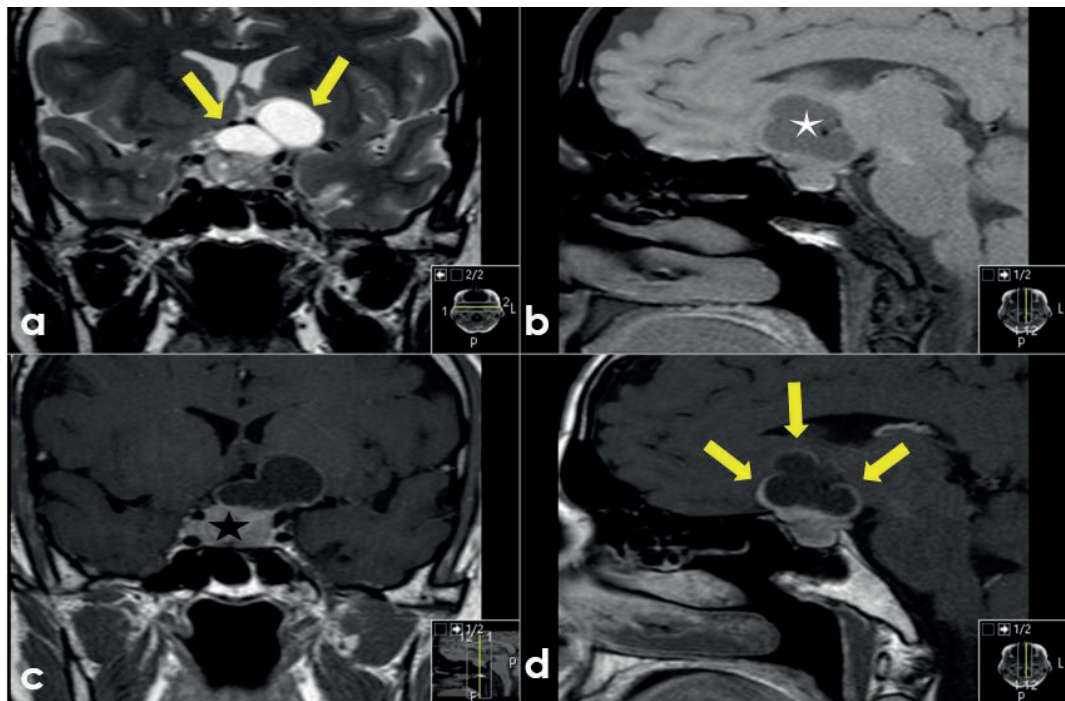


Figure 7. Pituitary adenoma in a 49-year-old female patient with a superior lobulated shape (yellow arrows in a and d), T1 hypointense (white star in b) cystic portion and homogeneously enhancing solid portion (black star in c).

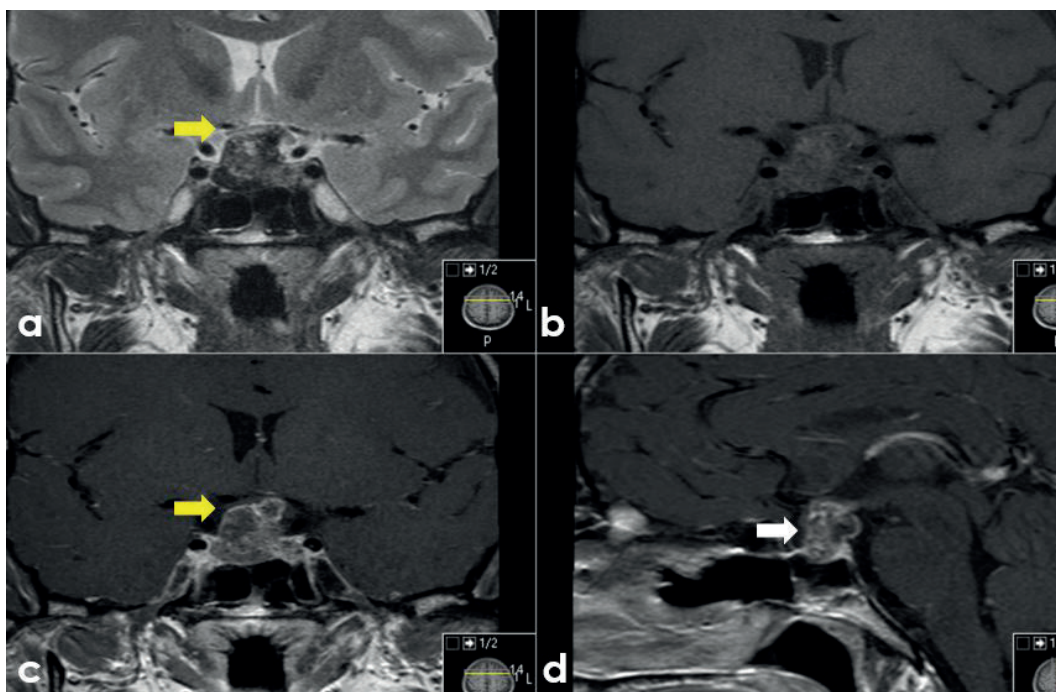


Figure 8. Craniopharyngioma in a 35-year-old male patient with a snowman-like shape and heterogeneously enhancing solid portion (white arrow in d). The superior portion compresses the optic chiasm (yellow arrows in a and c).

With respect to extension, compression of the third ventricle was more commonly observed in craniopharyngiomas (Fig. 3, 4 and 6) (70.7%, 29 of 41 patients) than in pituitary adenomas (Fig. 2, 5 and 7) ($p=0.003$). By contrast, cavernous sinus invasion was more commonly observed in adenomas (Fig. 1, 5 and 7) (22.2%, 10 of 45 patients) than in craniopharyngiomas (Fig. 6) ($p=0.011$).

In terms of the enhancement patterns of solid portions, most of the pituitary adenomas (94.3%) showed homogenous pattern (Fig. 1,

2, 5 and 7) (93.3%, 42 of 45 patients), while craniopharyngiomas showed reticular pattern (Fig. 3, 4, 6 and 8) (87.8%, 36 of 41 patients). There was statistically significant difference between groups ($p<0.001$).

The sensitivities and specificities of statistically significant MRI findings are summarized in Table 3. The enhancement pattern of solid component was found to be the most sensitive and specific MRI finding in distinguishing mixed solid-cystic pituitary adenomas from craniopharyngiomas involving both sellar and suprasellar regions.

Table 3. The sensitivities and specificities of statistically significant MRI findings.

Tumor	MRI findings	Sensitivity (%)	Spesifty (%)
Pituitary adenoma	Snowman-like shape	86	65
	Predominantly solid	62	53
	Cavernous sinus invasion	91	53
	Homogeneous enhancement	89	92
Craniopharyngioma	Superior lobulation	78	80
	Compressing third ventricle	67	72

DISCUSSION

Patients with pituitary adenoma or craniopharyngioma, involving both sellar and suprasellar regions, usually present with similar symptoms such as headache, visual disturbance, or hypopituitarism. Clinically, the differential diagnosis is not easy ^(2,9-11). On the other hand, the characteristic MRI findings of these tumours are well known, and their differential diagnosis is not problematic if they show typical imaging findings.

Pituitary adenomas with suprasellar extension typically have a “figure of eight” or “snowman” appearance with homogeneous enhancement ⁽⁴⁾. Craniopharyngiomas divide into two histological types, squamous-papillary and adamantinous, have been described in the literature, although in some cases they cannot be divided into distinct histological types ^(11,12). On MRI the typical features of squamous-papillary craniopharyngioma include a predominantly solid spherical tumour in the suprasellar region in adults ⁽¹¹⁾. The solid part shows heterogeneous but intense enhancement with small necrotic areas ⁽¹¹⁾. The cystic part contains a watery liquid that is hypointense on T1-weighted images and hyperintense on T2-weighted images ⁽¹¹⁾. On the other hand, adamantinous craniopharyngioma is a cystic or predominantly cystic, lobulate tumour, which is often observed in the intrasellar or suprasellar regions in children or adults ⁽¹¹⁾. On T1 weighted images, they have single or multiple hyperintense cysts with thin peripheral enhancing rims ⁽¹¹⁾. On T2-weighted images these cysts are either hyperintense or hypointense. Despite these well-known imaging findings, it is challenging to arrive at differential diagnosis in some cases ⁽¹³⁾.

Most pituitary adenomas arise from the pituitary gland and extend through the diaphragm sella up to the optic chiasm, and laterally to the

cavernous sinus; most craniopharyngiomas arise from the suprasellar region extending up to the third ventricle with lobulation and down to the intrasellar region ⁽¹³⁾. Concordant with this extension pattern, in our study, the cavernous sinus invasion was seen more commonly in adenomas, while the third ventricle compression was more common in craniopharyngiomas.

The cystic portions of the two tumours are believed to be composed of various entities: necrosis, haemorrhage, and cystic degeneration in pituitary adenoma ^(2,4); and a high protein concentration, cholesterol, or methaemoglobin in craniopharyngioma ⁽¹³⁾. In a previous study, Choi et al. ⁽¹³⁾ concluded that the signal intensity of the cystic fluid did not help in distinguishing adenomas from craniopharyngiomas. The results of the present study are concordant with this conclusion. T1-hyperintense cystic portion was more frequently observed in craniopharyngiomas but there was no statistically significant difference.

Homogeneous and reticular enhancement patterns were found to be key elements in the differential diagnosis of solid containing pituitary adenomas and craniopharyngiomas, respectively. Histopathological reviews of published studies suggest that the observed reticular enhancement pattern of solid containing craniopharyngiomas is caused by small regions of necrosis, keratin debris, or calcification ^(11,12). Although Choi et al. ⁽¹³⁾ reported a reticular enhancement pattern in all solid containing craniopharyngiomas in their study, homogeneous enhancement pattern was observed in five craniopharyngiomas in our study. One of them was adamantinous and the others were not specified. Squamous-papillary craniopharyngiomas presenting as homogeneously enhancing solid masses were reported by Sartoretti-Schefer et al. ⁽¹¹⁾ previously. In our study there were two squamous-papillary

craniopharyngiomas which showed reticular enhancement.

In conclusion, MRI features, including tumour shape, extent, characteristics and enhancement patterns of solid portions are useful in the differentiation of mixed cystic-solid pituitary adenoma and craniopharyngioma involving both sellar and suprasellar regions. The enhancement pattern of the solid component is the key finding.

Ethical Approval: This study was approved by the Kocaeli University Non-Invasive Clinical Research Ethics Committee (No: 2018/2072 / 26.12.2018).

Conflict of interest: There is no conflict of interest in our study.

Funding: No financial support was received in our study.

Etik Kurul: Bu araştırma Kocaeli Üniversitesi Girişimsel Olmayan Klinik Araştırmalar Etik Kurulu tarafından onaylanmıştır (Karar no: 2018/2072 / 26.12.2018).

Çıkar çatışması: Çalışmamızda herhangi bir çıkar çatışması bulunmamaktadır.

Finansal destek: Çalışmamızda finansal destek alınmamıştır.

REFERENCES

1. Doerfler, A. & Richter, Lesions within and around the Pituitary, G. Clin Neuroradiol 2008; 18: 5. <https://doi.org/10.1007/s00062-008-8001-0>
2. Johnsen DE, Woodruff WW, Allen IS, et al. MR imaging of the sellar and juxtaseilar regions. RadioGraphics 1991;11: 727e58. <https://doi.org/10.1148/radiographics.11.5.1947311>
3. Osborn AG. Pituitary macroadenoma. In: Osborn AG, editor. Diagnostic imaging: brain. Salt lake city, Utah: Amirsys; 2004. p. II-2-24-27.
4. Osborn AG. Pituitary apoplexy. In: Osborn AG, editor. Diagnostic imaging: brain. Salt lake city, Utah: Amirsys; 2004. p. II-2-28-31.
5. Hedlund GL. Craniopharyngioma. In: Osborn AG, editor. Diagnostic imaging: brain. Salt lake city, Utah: Amirsys; 2004. p. II-2-32-35.
6. Cappabianca P, Cirillo S, Alfieri A, et al. Pituitary macroadenoma and diaphragma sellae meningioma: differential diagnosis on MRI. Neuroradiology 1999;41:22e6. <https://doi.org/10.1007/s002340050698>
7. Van Effenterre R, Boch AL. Craniopharyngioma in adults and children: a study of 122 surgical cases. J Neurosurg 2002;97:3e11. <https://doi.org/10.3171/jns.2002.97.1.0003>
8. Kim JE, Kim JH, Kim OL, Paek SH, Kim DG, Chi JG, Jung HW. Surgical treatment of symptomatic Rathke cleft cysts: clinical features and results with special attention to recurrence. J Neurosurg 2004;100(1):33-40.
9. Poussaint TY, Barnes PD, Anthony DC, et al. Hemorrhagic pituitary adenomas of adolescence. AJNR Am J Neuroradiol 1996;17:1907e12.
10. Kucharczyk W, Peck WW, Kelly WM, et al. Rathke cleft cysts: CT, MR imaging, and pathologic features. Radiology 1987;165:491e5. <https://doi.org/10.1148/radiology.165.2.3659372>
11. Sartoretti-Schefer S, Wichmann W, Aguzzi A, et al. MR differentiation of adamantinous and squamous-papillary craniopharyngiomas. AJNR Am J Neuroradiol 1997;18:77e87.
12. Eldevik OP, Blaivas M, Gabrielsen TO, et al. Craniopharyngioma: radiologic and histologic findings and recurrence. AJNR Am J Neuroradiol 1996;17:1427e39.
13. S. H. Choi, B. J. Kwon, D. G. Na, J-H Kim, M. H. Han, K-H Chang, Pituitary adenoma, craniopharyngioma, and Rathke cleft cyst involving both intrasellar and suprasellar regions: differentiation using MRI. Clin Radiol. 2007 May; 62(5): 453-62. <https://doi.org/10.1016/j.crad.2006.12.001>